Comparison of measured and EF5-r derived N₂O fluxes from a spring-fed river.

TIM. J. CLOUGH[*], JANET E. BERTRAM[*], ROBERT R. SHERLOCK[*], ROBERT L. LEONARD[*] and BARBARA L. NOWICKI[†]

[*]*Agriculture & Life Sciences Division, PO Box 84, Lincoln University, Canterbury, New Zealand,* [†]*College of the Environment and Life Sciences, University of Rhode Island, Kingston, RI 02881, USA*

Correspondence: Tim. J. Clough, Agriculture & Life Sciences Division, PO Box 84, Lincoln University, Canterbury, New Zealand, fax +64 3 325 3607; +64 3 325 2811 ext8360, e-mail: clought@lincoln.ac.nz

Running title: River N₂O fluxes and EF5-r.

Abstract

There is considerable uncertainty in the estimates of indirect N_2O emissions as defined by the Intergovernmental Panel on Climate Change's (IPCC) methodology. Direct measurements of N_2O yields and fluxes in aquatic river environments are sparse and more data are required to determine the role that rivers play in the global N_2O budget.

The objectives of this research were to measure the N_2O fluxes from a spring-fed river, relate these fluxes to the dissolved N_2O concentrations and NO_3–N loading of the river, and to try and define the indirect emission factor (EF5-r) for the river.

Gas bubble ebullition was observed at the river source with bubbles containing 7.9 µL N_2O L^{-1}. River NO_3–N and dissolved N_2O concentrations ranged from 2.5 to 5.3 mg L^{-1} and 0.4 to 1.9 µg N_2O-N L^{-1} respectively with N_2O saturation reaching 404%. Floating headspace chambers were used to sample N_2O fluxes. N_2O–N fluxes were significantly related to dissolved N_2O–N concentrations ($r^2 = 30.6$) but not to NO_3–N concentrations. The N_2O–N fluxes ranged from 38-501 µg m^{-2} h^{-1}, averaging 171 µg m^{-2} h^{-1} (± Std. Dev. 85) overall. The measured N_2O–N fluxes equated to an EF5-r of only 6.6% of that calculated using the IPCC methodology, and this itself was considered to be an over-estimate due to the degassing of antecedent dissolved N_2O present in the groundwater that fed the river.

Introduction

Atmospheric concentrations of N_2O, a greenhouse gas (GHG), have increased since pre-industrial times to the present (Prinn *et al.*, 1990, Rockmann *et al.*, 2003) and continue to rise at 0.2-0.3% yr^{-1} (Nevison, 2000b). Due to the lack of any stabilization in atmospheric GHG concentrations, parties to the United Nations Framework Convention on Climate Change (UNFCC) negotiated the Kyoto Protocol. This protocol sets targets for participating countries to reduce or take responsibility for their excess GHG emissions. An obligation of the parties that are signatories to the UNFCCC and the Kyoto protocol is the development and publication of an annual national inventory of all anthropogenic GHG emissions and removals. The IPCC methodology predicts that in many countries N_2O will comprise at least 10% or more of the aggregate GHG emissions (Nevison, 2000b); in New Zealand's case, N_2O emissions comprise 17% of the total aggregated GHG emissions per annum (New Zealand Climate Change Office, 2004).

Guidelines on how to construct inventories have been prescribed by the Intergovernmental Panel on Climate Change (IPCC) and include a number of "default" assumptions and data for use in the calculation of GHG emissions and removals (IPCC, 1997). The IPCC guidelines divide agricultural N_2O sources into three categories: direct emissions from agricultural land, emissions from animal waste systems, and indirect emissions associated with nitrogen (N) that is removed in biomass, volatilized, leached, or exported from the agricultural land (Mosier *et al.*, 1998). The aim of this methodology is to provide a standardized framework to account completely for the annual N_2O production associated with agricultural practice on a per country basis. Each of the three N_2O source categories typically contributes an equal 1/3 share of the total estimated agricultural N_2O source (Nevison, 2000b). However, approximately 2/3 of the uncertainty in the total

agricultural N_2O source is due to the wide range of estimates for indirect N_2O emissions (Nevison, 2000b).

The total global N_2O source from agricultural soils stands at 6.3 Tg N yr^{-1}(Mosier *et al.*, 1998). Indirect emissions account for 2.1 Tg N yr^{-1} of this total; nitrogen leaching and runoff dominate the indirect emission sources accounting for over 75% of estimated indirect emissions (Mosier *et al.*, 1998, Nevison, 2000b). Biological cycling of both the natural and anthropogenic N through aquatic ecosystems produces emissions of N_2O via nitrification and denitrification. N_2O production allied to N leaching and runoff is defined by the IPCC methodology as follows (IPCC, 1997, Mosier *et al.*, 1998):

NLEACH = (NFERT+ NEX) * FRACLEACH

N2O(L) = NLEACH * EF5

Where NLEACH (kg N yr^{-1}) is the mass of fertilizer and manure N lost through leaching and runoff per annum, NFERT (kg N yr^{-1}) the mass of fertilizer used per annum, NEX (kg N yr^{-1}) the mass of manure N excreted by livestock per annum, and FRACLEACH the fraction of the fertilizer and manure N lost to leaching and surface runoff (range 0.1 - 0.8). The N_2O emissions due to agricultural N loss through leaching and runoff (N2O(L)) are calculated by multiplying NLEACH by the emission factor (EF5) for leaching and runoff. The value of EF5 is the sum of the N_2O emission factors for N_2O losses from i) groundwater and surface drainage (EF5-g = 0.015 kg N_2O–N per kg NLEACH), ii) rivers (EF5-r = 0.0075 kg N_2O–N per kg NLEACH), and iii) coastal marine areas (EF5-e = 0.0025 kg N_2O–N per kg NLEACH). The rationale behind the development of the default values for EF5-g, EF5-r and EF5-e have been previously described (Mosier *et al.*, 1998, Nevison, 2000b).

As noted above, current estimates of the total agricultural sourced N_2O emissions equate to 6.3 Tg N yr^{-1} which is greater than the observed atmospheric increase of 3.9 Tg N yr^{-1}. A simple explanation for this is that the IPCC methodology over-estimates the anthropogenic source (Nevison, 2000b). There is considerable discussion in the literature regarding the appropriate magnitude of the default factors for FRACLEACH and the components of EF5, with suggestions for possible improvements to the assumptions and the magnitudes of the default factors (Groffman *et al.*, 2000, Nevison, 2000b, Groffman *et al.*, 2002, Reay *et al.*, 2003). Actual measurements of N_2O yields in aquatic river environments are sparse (Nevison, 2000b, Cole & Caraco, 2001) and an assumption commonly made is that the N_2O yield is 0.5% for both nitrification and denitrification (Mosier *et al.*, 1998, Seitzinger & Kroeze, 1998). Cole and Caraco (2001) measured N_2O fluxes from the Hudson river and compared these with modelled estimates, determined using the model of Seitzinger and Kroeze (1998). They found the measured fluxes to be considerably lower than the modelled fluxes, as was the case for four out of seven other rivers, where measured values were also lower than modelled values. In the case of the Hudson river, the assumptions used in the model (Seitzinger & Kroeze, 1998) over-estimated denitrification and nitrification rates. More data are required to determine the role rivers play in the N_2O budget (Cole & Caraco, 2001, Groffman *et al.*, 2002).

This study presents N_2O flux data and associated river measurements from a spring-fed river that flows through an agricultural landscape. The data are used to examine the relationship between the measured fluxes and a component of the EF5 emission factor, EF5-r.

Materials and Methods

This study was carried out on the LII river, situated in the Canterbury region of the South Island, New Zealand (Fig. 1). In the Canterbury Plains area confined and unconfined aquifers

carry water from the Southern Alps eastwards towards the Pacific Ocean. Aquifers are primarily composed of gravels with small proportions of finer textured sands and silts. The lower the percentage of sand and silt the greater the permeability and yield of the aquifer. Aquifers high in sand and silt are lower yielding and are referred to as aquitards (Bowden, 1986). The uppermost water bearing layers over the inland plains have a high permeability and are referred to as unconfined aquifers. Rain water and river waters move into the unconfined aquifers and travel laterally towards the East Coast recharging the unconfined aquifers. Groundwater is vulnerable to contamination especially from associated land uses over the aquifers. In the coastal area around the city of Christchurch (Fig. 1) the groundwater flowing at shallow depth towards Christchurch city meets confining aquitards, and water is forced both below the aquitard and above the aquitard into the near-surface gravels and the spring-fed rivers (Bowden, 1986). Base flows in these spring-fed rivers are derived from the re-surfacing shallow groundwater (Bowden, 1986).

The LII is a spring-fed river, 12 km long, commencing 10 m above sea level near Lincoln township (Lat./Long. 43.64673S, 172.49677E), and flows in a south westerly direction for a distance of 12 km whereupon it discharges into Lake Ellesmere (Fig. 1). Four sampling sites were selected for this study. These were located evenly along the length of the river and had easy road access. Sites 1, 2, 3 and 4 were located at the 0, 4.4, 7.7 and 10 km from the spring. The LII river flows through land under agricultural stewardship that includes orchards, dairy, and sheep farms. The watershed area and N loading of the watershed are not readily definable. However, drainage ditches from the agricultural lands discharge into the LII at regular intervals. There are no direct point sources of effluent, such as dairy waste ponds, discharging into the LII. The river's mean gradient was 0.08%.

River flow measurements were performed using the velocity-area method (Mosley *et al.*, 1992, Davie, 2003). In brief this entailed calculating the trapezoidal cross-sectional area

of the river and measuring the river velocity with a timed float. River depth was monitored at sites 3 and 4 using pre-existing flow gauges that had been installed by the regional council. Meteorological data was collected at the Lincoln University climate station, a distance of 3 km from site 1.

Floating chambers were constructed from round polypropylene "cake" containers (Decor®, product No. 350, Australia). The container lids were discarded and the containers inverted so that the open side formed the chamber base. The containers were shaped like a conical frustrum (radii of 10.1 and 11.3 cm at the chamber roof and water surface respectively; an internal height from chamber roof to water surface of 11.7 cm). A styrofoam annulus (8.5 cm wide, 11.7 cm deep) was attached around the chamber. The polypropylene chamber projected 1.5 cm into the water when floating on the river surface. This was in addition to the internal chamber height of 11.7 cm. The resulting headspace volume of the floating chamber was 4.2 L. A rubber septum was placed in the roof of the plastic chamber to facilitate headspace gas sampling. The septa were from blood evacuation tubes (BD, Dickinson, NJ.). Laboratory testing of the floating chambers showed no N_2O production or consumption over a 60 minute period. Testing of the floating chambers on the LII river showed that N_2O concentrations increased in a linear manner for up to 60 minutes. This time was well in excess of the 15 minute sampling times used in the study (see below).

Unless otherwise stated 10 replicate chambers were used at each site during sampling of the river surface gas fluxes. To determine the river surface gas fluxes the chambers were placed on the water surface, linked with 1 m lengths of string and allowed to drift freely with the river current. A terminal chamber was linked via string to an observer on the river bank who walked alongside the river. Chambers were deployed at the same position, and in the same sequence, on each sampling occasion. Chamber capture was performed after 15 minutes

by gently pulling the chambers back to quiet water alongside the bank, where gas sampling occurred.

Glass syringes equipped with three way large bore stopcocks (Part No. 2C6201, Baxter Healthcare Corp., Deerfield IL.) were used to take gas samples while the chambers remained floating on the river surface. A gas sample of 10 mL was taken from the headspace chamber and flushed to waste, twice. On the third occasion the 10 mL sample was injected into a previously evacuated (<0.01 atmosphere) 6 mL glass sample tube with a screw cap and rubber septum (Exetainer®, Labco Ltd., UK.), creating an internal over-pressure. Ambient air gas samples were also taken at each site when chamber headspace samples were obtained.

Gas samples were analysed using a gas chromatograph (8610, SRI Instruments, CA.) interfaced to a liquid autosampler (Gilson 222XL, Middleton, WI.). The autosampler had been specially modified for gas analysis by substituting a purpose-built (PDZ-Europa, Crewe, UK) double concentric injection needle for the usual liquid level detector and needle. This enabled the entire gas sample to be flushed rapidly from its septum-sealed container (6 mL Exetainer®) into the GC.

The GC configuration was similar to that used by Mosier and Mack (1980) and included two 0.3 cm OD stainless steel columns packed with Haysep Q connected in series, oxygen-free dry nitrogen carrier gas (40 mL min^{-1}), and a ^{63}Ni electron capture detector at 320 ^{o}C. Gas samples were analysed within 1 to 2 days of sampling. Immediately prior to analysis the over-pressurised samples were all brought to ambient atmospheric pressure, using a double-ended hypodermic needle. One end of the needle was placed at a constant depth (0.5 cm) just below the surface of some water in a small beaker while the other end pierced the Exetainer® septum. A brief flow of bubbles resulted and when these ceased, the gas in the Eexetainer® was at ambient air pressure. Dissipating the excess gas pressure through the water medium not only gave a visual indication of when the samples were at

ambient air pressure, it also avoided any potential contamination of the sample with ambient air. Reference gases (0.363 to 35.2 μL L^{-1}, BOC Ltd. Auckland) were prepared following the same over pressure-equilibration procedure as described above. Detection limits for N_2O analysis were considered significant if concentrations were 0.01 μL L-1 > than the ambient concentration.

Water samples for measurement of dissolved gases were collected in 500 mL glass reagent bottles. Bottles were first rinsed with river water and then submerged ca. 20 cm below the water surface and allowed to fill completely. Then a glass stopper was inserted, prior to the bottle's removal from the stream and its placement into a styrofoam insulated box, where it was stored until arrival back at the laboratory. River and air temperatures were measured *in-situ* using a portable pH meter fitted with a combination pH and temperature probe (HI9025, Hanna Instruments, Italy).

Gas ebullition at the spring was collected by placing an inverted plastic funnel, connected to a 2 L volumetric glass flask full of water, below the water surface. As the gas was collected the water in the flask was displaced. After 2 L of gas was collected a rubber septum was used to seal the flask prior to transporting it back to the laboratory for gas analyses.

Back in the laboratory the river water samples were subsampled and analyzed for dissolved oxygen (DO), inorganic–N (NH_4–N, NO_2–N, NO_3–N), dissolved total organic carbon (TOC), electrical conductivity (EC), pH, and dissolved N_2O. DO was measured using the iodometric titration method with an azide modification (Clesceri *et al.*, 1998). Inorganic-N concentrations were determined using colorimetric methods and an auto-analyser with a detection limit for NO_3-N L^{-1}, NO_2-N L^{-1} and NH_4-N L^{-1} of 0.10, 0.01, and 0.01 mg L^{-1} respectively (Alpkem FS3000 twin channel analyser; application notes P/N A002380 and P/N A002423). Dissolved TOC was calculated from the difference between dissolved total carbon

(TC) less dissolved inorganic carbon (TIC), i.e. TOC = TC-TIC. Dissolved carbon analyses were performed with a Shimadzu TOC-Analyser fitted with a Shimadzu ASI-5000A autosampler. The detection limit for dissolved organic carbon and inorganic was 1 mg L^{-1}. A conductivity meter (CDM83, Radiometer, Copenhagen) was used to measure the EC of the water samples.

Concentrations of dissolved gases in the river water samples were analysed according to Davidson and Firestone (1988) with appropriate Bunsen coefficients obtained for N$_2$O (Young, 1981). Initially a microbial inhibitor (mercuric chloride) was added to the water sample (Kirkwood, 1992). However, use of the inhibitor was discontinued when tests showed no difference in the dissolved N$_2$O results between inhibited and non-inhibited samples. Nitrous oxide equilibrium concentrations (nmol L^{-1}) in the river water were determined using an atmospheric N$_2$O partial pressure of 3.1 x10^{-7} atm and the appropriate solubility coefficient for N$_2$O (mol L^{-1} atm^{-1}) for the temperature of the water sampled (Weiss & Price, 1980)). Dissolved N$_2$O concentrations were then converted to units of µg N$_2$O-N L^{-1}.

An N$_2$O–N flux was calculated for the river reach between sites 1 and 4, according to the IPCC methodology and assumptions, using the following data: a NO$_3$–N concentration of 2.8 mg L^{-1}, a river flow of 3.41 m^3 s^{-1}, and an average river width of 10 m with a length of 10,000 m. A theoretical N$_2$O flux (F_{N2O}; mole m^{-2} s^{-1}) was also calculated using the stagnant-two-film approach (Liss & Slater, 1974):

$$F_{N2O} = -V_W^{N2O}([N_2O] - \frac{p_{N2O}}{K_H}$$

Where K_H was the Henry's Law constant (atm. m^3. mole^{-1}), p_{N2O} the partial pressure of N$_2$O in the atmosphere (atm.), $[N_2O]$ the concentration of N$_2$O in the water (mole m^{-3}), and V_W^{N2O} the transfer velocity (m s^{-1}). The value of V_W^{N2O} was estimated from the transfer velocity of a

reference gas, oxygen, as $V_W^{N2O} = 0.913 \times V_W^{O2}$ (Holmen & Liss, 1984). Transfer velocity of

oxygen was assigned as discussed below in the results and discussion sections.

River surface N_2O flux measurements and associated water samplings were carried

out on the LII river from autumn through to spring. Surface N_2O flux measurements were

taken on the 3rd, 17th, and 31st May, 17th June, 8th July, 16th August, and the 10th September.

Dissolved N_2O concentrations were measured on the same dates as the N_2O flux

measurements and also on the 5th and 26th of April, and the 28th of July. Inorganic-N and

dissolved carbon sample dates were the same as for the dissolved N_2O samples but also

included the 5th and 19th of March, and 1st of October. To establish if these results were

representative of other spring-fed rivers, N_2O flux and NO_3–N measurements were also taken

from another agriculturally influenced spring-fed river approximately 10 km to the north of

the LII, the 'Halswell'; and two other spring-fed rivers the 'Avon' and the 'Heathcote' that

flow through the major urban centre of Christchurch, approximately 25 km away (Fig. 1).

These other rivers were sampled on one occasion (18th August) using the same methods.

Results

Meteorological data and river chemistry

Average wind run, and air temperatures over the study period were 342 km d^{-1} (range

84 to 689 km d^{-1}) and 9.2 ^{o}C (range 4.2 to 14.5 ^{o}C) respectively (Fig. 2). Maximum daily

rainfall occurred in August with a maximum rainfall of 65 mm on August 6th (Fig. 2). The

river flow ranged from 2.98 to 4.07 m[3] s^{-1} with the respective residence times of the water in

the LII river ranging from 10.2 to 7.5 h (Table 1)

River water pH ranged from 6.2 to 7.6, and increased from site 1 (the source) to site 4

($p < 0.05$). Site 1 had significantly lower EC values than the other sites ($p < 0.01$), averaging

160 μS cm^{-1} [± Std. Dev. 8]. The average EC values at sites 2, 3 and 4 averaged 190 μS cm^{-1}

[± Std. Dev. 20] with no differences between these sites. At sites 2 to 4 the maximum EC values (259 µS cm^{-1}) occurred immediately after a large rainfall event on 6th August. No increase in EC was measured at site 1 at this time. Water temperatures were stable at site 1 (13.1 ^{o}C [± Std. Dev. 0.3]) and differed significantly from sites 2 to 4 ($p < 0.01$), where changes in river water temperature (range 8.1 - 13.0 ^{o}C) were driven by changes in air temperature. Correlations (r) between air temperature and water temperature for sites 2, 3 and 4 were 0.91, 0.87 and 0.89 respectively. At site 1 the DO concentrations averaged 6.9 mg O$_2$ L^{-1} [± Std. Dev. 0.3] and were significantly lower ($p < 0.05$) than concentrations at sites 2 to 4 where DO concentrations averaged 8.5 mg O$_2$ L^{-1}. At sites 2 to 4 the DO concentrations decreased by 2 mg O$_2$ L^{-1} immediately following the high rainfall event in August for several days before returning to their previous levels.

Concentrations of NO$_3$–N in the river at sites 1, 3 and 4 were quite stable throughout the study averaging 2.8 mg L^{-1} and remained within the range of 2.3 to 3.3 mg L^{-1} (Table 2). However, at site 2 concentrations of NO$_3$–N were higher ($p < 0.01$) and ranged from 3.4 to 5.2 mg L^{-1} (Table 2). The NH$_4$–N concentrations in the LII were an order of magnitude lower and constantly < 0.2 mg L^{-1} (Table 2) with peak concentrations occurring at the start of the study in March, mid-April for (sites 2 -4), mid-winter (all sites), and following the high rainfall event in mid-August (sites 2-4). Concentrations of NO$_2$–N were generally below the level of detection (0.01 mg L^{-1}) except for sites 3 and 4 following the high rainfall event in mid-August when NO$_2$–N concentrations were 0.02 and 0.04 mg L^{-1} respectively.

Total organic-C concentrations were approximately 3 mg L^{-1} at the start of the study and then decreased in early April to be < 2 mg L^{-1} where they stayed except for the rise in August following the high rainfall event when levels increased significantly at sites 2 - 4 (Fig. 3). Dissolved inorganic-C concentrations did not differ significantly between sites and were

lowest at the commencement of the study, mean concentrations ranging from 13 -14 mg L^{-1} (Fig. 3).

Dissolved N$_2$O and N$_2$O fluxes

Gas ebullition was observed from the sediment at the spring (site 1). The concentration of N$_2$O in the evolved gas bubbles, measured in May, was 7.9 µL L^{-1}. The average concentrations of dissolved N$_2$O-N at the four sites, in the LII river, ranged from 0.43 to 1.89 µg N$_2$O-N L^{-1} and decreased ($p < 0.01$) with increasing distance from the spring (Table 3). Significant differences between sites did not occur until 17th of June when the dissolved N$_2$O at sites 1 and 2 were significantly higher ($p < 0.01$) than at sites 3 or 4. This pattern continued until the end of the study. When averaged across all sampling times, the values of dissolved N$_2$O at sites 1, 2, 3, and 4 were 1.36 (0.40), 1.33 (0.41), 0.74 (0.23), and 0.67 (0.24) µg N$_2$O-N L^{-1} respectively (numbers in brackets are standard deviations). These represent N$_2$O saturation levels for sites 1, 2, 3, and 4 of 404 (119), 395 (118), 223 (68), and 201 (74) %, respectively (numbers in brackets ± Std. Dev.).

Ratios of dissolved N$_2$O–N: NO$_3$–N ranged from 0.00015 to 0.00067 across all sampling dates (Table 3). The mean ratio N$_2$O–N: NO$_3$–N, over all sampling dates, decreased from site 1 to 4 with values of 0.00049 (±0.00011 Std. Dev.) to 0.00022 (±0.00007 Std. Dev.) respectively. A regression analysis of this ratio against distance downstream from the site 1 was highly significant ($r^2 = 59.2\%$, $p < 0.01$).

The N$_2$O–N fluxes, from individual sampling dates, ranged from 38-501 µg m^{-2} h^{-1}. Mean fluxes of N$_2$O–N at sites 1 and 2 were higher than those at sites 3 and 4 for the majority of sample dates (Table 4). When averaged over the entire period of the study the N$_2$O–N fluxes from sites 1, 2, 3 and 4 were 197(88), 241(86), 136(49), and 110(29) µg m^{-2} h^{-1} respectively (numbers in brackets ± Std. Dev.), with the average fluxes from sites 1 and 2

significantly higher ($p < 0.01$) than those from sites 3 and 4. The overall mean N_2O–N flux was 171 µg m^{-2} h^{-1} (± Std. Dev. 85). The N_2O fluxes and NO_3–N concentrations measured from the LII river were typical of those measured from the other local agricultural and urban spring-fed rivers (Fig. 4a). Of the other rivers, which flow through Christchurch, the Avon river had the highest N_2O–N flux (973 µg m^{-2} h^{-1}), 1 km from its source, and the lowest NO_3–N concentrations (Fig. 4a).

The mean N_2O–N fluxes and the mean dissolved N_2O concentrations showed no relationship to the corresponding NO_3–N concentrations (Fig. 4a, 4b). The regression between the mean dissolved N_2O concentrations versus the mean N_2O–N fluxes, for all sites, was significant ($r^2 = 0.31$, $p < 0.05$) and further improved if the additional data points of zero flux with a mean equilibrium N_2O-N concentration of 0.34 µg N_2O-N L^{-1} were included ($r^2 = 0.58$, $p < 0.01$, Fig. 5). If data from site 1 were excluded, on the basis that some of the N_2O in the measured flux was almost certainly due to ebullition events, then the regression improved to $r^2 = 0.74$. Predicted N_2O fluxes, based on dissolved N_2O concentrations are plotted in Figure 5 based on oxygen transfer velocities of 0.5×10^{-4} m s^{-1} and 2.5×10^{-4} m s^{-1} and are discussed below.

The gross advective daily discharge of dissolved N_2O downstream from site 4 equalled 0.20 kg dissolved N_2O–N d^{-1}, based on an N_2O concentration of 0.67 µg N_2O–N L^{-1} and a mean flow of 3.41 m^3 s^{-1}. This was less than the daily N_2O–N flux of 0.41 kg N_2O–N d^{-1} evolved from the 10 km reach of river leading to site 4, based on a mean river width of 10 m and a mean N_2O–N flux of 171 µg m^{-2} h^{-1}. The daily discharge of NO_3–N downstream from site 4, equated to 825 kg NO_3–N d^{-1}, based on the mean NO_3–N concentration of 2.8 mg L^{-1} and a mean flow of 3.41 m^3 s^{-1}. Thus the daily mean loss of N_2O–N was insignificant compared to the NO_3–N lost, equalling just 0.07% of the NO_3–N discharged from site 4.

The IPCC default value for EF5–r (0.0075 kg N_2O kg^{-1} NO_3–N) yielded a calculated daily flux of 6.2 kg N_2O–N d^{-1} from the LII river whereas the average measured flux was 0.41 kg N_2O–N d^{-1} i.e. just 6.6% of that calculated using the IPCC methodology.

Discussion

River chemistry

The values of pH, EC, and DO in the LII were typical of natural freshwater systems (Dojlido & Best, 1993). The measured values of temperature, pH, EC, TOC and DO were relatively constant at site 1 indicating that water chemistry at this site was predominately influenced by the water discharged from the spring and relatively unaffected by the climatic changes, physical, and/or biological inputs that subsequently influenced the LII river chemistry downstream from site 1. The observed increases in NH_4–N at site one between April and August are not readily explainable but could be related to high populations of aquatic birdlife resident there during this time.

The high rainfall event in August followed a period of snowfall and the surrounding land was water-saturated. Due to the intensity of the rainfall event, overland flow of water occurred. This accounted for the increased levels of NH_4–N, EC and TOC, and the observed decrease in DO following the rainfall event. Interestingly the NO_2–N levels also increased at this time, possibly indicating a period of denitrifying activity following the high rainfall event. Other studies have also found elevated TOC concentrations occurring from surface or near surface runoff following storm events (Inamder *et al.*, 2004). Dissolved oxygen levels indicated that the LII was generally well oxygenated throughout the study period.

Dissolved N_2O and NO_3–N

The higher NO_3–N concentrations at site 2 were atypical. Further NO_3–N addition(s) must have occurred either from drainage tributaries or from further groundwater flow(s), with high NO_3–N concentration, between sites 1 and 2. Flows at sites 1 and 2 were not gauged but it was readily apparent, visually, that the river flow was greater at site 2 than at site 1. Additional work needs to be performed to clarify where and how this NO_3–N input occurs.

Assuming nil production of N_2O in the river, and assuming no other inputs, there should have been a decrease in the dissolved N_2O concentration, due to N_2O degassing from the water surface between sites 1 and 2. This was not observed despite the relatively high N_2O fluxes measured. Thus additional inputs of N_2O occurred either via *in-situ* nitrification/denitrification processes or the further addition of water(s) containing high levels of dissolved N_2O. Additional N_2O inputs could have occurred as for NO_3–N, as described above. Dowdell *et al.* (1979) measured dissolved N_2O in agricultural drainage waters. Alternatively in-stream production of N_2O could also have occurred due to microbial processes. Denitrification as a source of N_2O cannot be ruled out, despite the well oxygenated status of the LII, because it could have been occurring at the interface between the anaerobic sediments and water-body (Petersen *et al.*, 2001).

The decrease in both the NO_3–N and dissolved N_2O–N concentrations between sites 2 and 3 could, again, have been due to dilution from water with lower NO_3–N and dissolved N_2O–N concentrations, or via consumption processes. Further additions of water to the LII between sites 2 and 3 occurred through a multitude of drainage ditches.

The observed drop in the dissolved N_2O concentration, between sites 2 and 3, was not maintained between sites 3 and 4, a distance of 2.3 km, despite the water still being over-saturated with N_2O ($> 200\%$). This suggests that the N_2O flux from the river surface was matched by N_2O inputs over this reach of the river. Again further work is required to identify the source(s) and scale of the N_2O inputs. It was noticeable that over this stretch of the river

that the geometry of the river became shallower and broader thus there was a larger sediment area exposed per unit volume of water. This may have contributed to more anaerobic sediment surfaces for *in-situ* N_2O production (Petersen *et al.*, 2001). Alternatively it may be that the NO_3-N measurements were not sensitive enough to detect the possible transformation of NO_3-N to N_2O-N. As noted above the daily advective loss of N_2O-N from site 4 was only 0.07% of the NO_3-N discharged. Assuming the same fraction of NO_3-N was being transformed to N_2O-N would require a decrease in the NO_3-N concentration of only 0.002 mg NO_3-N L^{-1}. This is well below the level of detection for the NO_3-N analyses.

N_2O fluxes and IPCC calculations

As observed from the ebullition events and high levels of N_2O saturation in the water it can be concluded that N_2O was introduced into the river at its source, site 1. Furthermore, dissolved N_2O was probably introduced into the LII along the reach from site 1 to site 2 via other tributaries or possibly further groundwater flow. The EF5-g component of EF5 was formulated on the basis that the N_2O formed in surface soils undergoes transport with leaching water to the groundwater and eventually degasses to the atmosphere by upward diffusion or following entry of groundwater into surface waters (Mosier *et al.*, 1998). A study by Reay *et al*. (2003) demonstrated how rapidly N_2O degassing from drainage waters can occur. It is apparent that degassing of N_2O already present in the groundwater, hereafter referred to as antecedent N_2O, contributed significantly to the N_2O fluxes measured in our study, especially between sites 2 and 3, as can be seen from the following calculation. Based on an LII river velocity of 0.28 m s^{-1} it requires 3.3 h for river water to travel between sites 2 and 3, through an estimated area of 33000 m^2. Assuming further, a river flow of 3 m^3 s^{-1}, and the drop in dissolved N_2O was as measured i.e. 1.34 to 0.67 µg N_2O–N L^{-1}, then the calculated N_2O–N flux equates to 219 µg m^{-2} h^{-1}, which is of quite similar magnitude to the

actual mean fluxes measured at sites 2 and 3 of 136 μg m^{-2} h^{-1} (49 Std. Dev.) and 110 μg m^{-2} h^{-1} (29 Std. Dev.) respectively. Thus in this study where the LII river is fed from an aquifer, and is of a relatively short length, degassing of antecedent N_2O appears to be a dominant component of the N_2O emissions.

The average N_2O–N flux from the LII was intermediate in magnitude compared with other studies where *in-situ* N_2O surface fluxes have been physically measured from streams or rivers. Nitrous oxide fluxes from the Hudson river, Platte river, and a stream exiting a rice paddy area have been recorded as having N_2O–N fluxes of 6, 6, and 240-56580 μg N_2O–N m^{-2} h^{-1} respectively with corresponding NO_3–N levels of 0.6, 0.1-11.2, and 20 mg NO_3–N L^{-1} (MacMahon & Dennehey, 1999, Hasegawa *et al.*, 2000, Cole & Caraco, 2001). The ratios of N_2O–N: NO_3–N measured in this study are within the range of values reviewed and quoted by Nevison (2000a) who found values of 0.0002 -0.0044 (groundwater) and 0.0005 - 0.01 (drainage ditches), with no strong difference between groundwater and drainage ditches. The lack of any significant relationships between the NO_3–N concentrations dissolved N_2O–N, and the N_2O–N fluxes supports the suggestion that degassing of the antecedent N_2O–N load occurred without any concurrent transformation of the NO_3–N load (Reay *et al.*, 2003).

We have made the assumption that all of the NO_3–N in the LII was anthropogenic and calculated our "IPCC flux" using the EF5-r component of 0.0075. Our average measured N_2O–N flux was only 6.6% of that calculated using the IPCC approach. In other words for the LII an EF5-r factor of 0.0005 was more appropriate. This is a large discrepancy and the possibility that our measurement method introduced significant bias needs to be considered. Our measured fluxes could possibly have underestimated the actual fluxes due to the headspace methodology used. The gas transfer velocity of a gas from water to the atmosphere is affected by both water turbulence and wind speed (MacIntyre *et al.*, 1995). Thus the water

surface turbulence under our headspace enclosures may have varied compared with that of the surrounding river. Likewise the lack of wind inside the headspace may also have caused lower fluxes; the wind run was significant (Fig. 2). In addition the bobbing motion of chambers on the water can create pressure fluctuations that may also influence the gas transfer velocity (MacIntyre *et al.*, 1995).

Predicted N_2O emissions, based on dissolved N_2O concentrations, were presented in Figure 5 using 2 arbitrary values of the transfer velocity. These values were chosen so that the predicted fluxes represented the upper and lower limits of the measured fluxes. The majority of the measured headspace flux data fell between these two arbitrary boundaries. The values of V_W^{N2O} used in Figure 5, 2.28 x10^{-4} and 3.65 x10^{-5} m s^{-1}, correspond to oxygen transfer velocities of 2.5 x10^{-4} and 4.0 x 10^{-5} m s^{-1} respectively. As noted above transfer velocity is dependent on wind flow. Out wind speed data was collected at a height of 10 m with the average daily wind run equal to 342 km d^{-1} or 3.95 m s^{-1}. Interpolating the data of Liss (1973) provides an oxygen transfer velocity of approximately 5 x10^{-5} m s^{-1} at this wind speed. However, it is well recognized that wind speed decreases closer to the water surface via the usual logarithmic profile (Israelsen & Hansen, 1962). Conversion of the wind speed at 10 m (Z_1) to a wind speed at a height of 0.05 m above the water surface (Z_2) can be achieved using:

$$\frac{U_1}{U_2} = \log\left(\frac{Z_1}{Z_0}\right) \div \log\left(\frac{Z_2}{Z_0}\right)$$

Where Z_0 equals the "effective roughness height", assumed to be 0.01 m, and U_1 and U_2 are the respective wind speeds at heights Z_1 and Z_2. Thus the average wind speed at 0.05 m above the average water is calculated to equal 0.92 m s^{-1}. Given that this is the more likely wind speed at the water surface in our study then the transfer velocity for oxygen also decreases. If the data of Liss (1973) is extrapolated this value is approximately1 x10^{-5} m s^{-1}. These

calculations suggest that our measured fluxes and methodology used were in general agreement with theoretically derived fluxes. These theoretically derived fluxes were dependent on the value of the oxygen transfer velocity assumed which was in turn highly dependent on wind speed. In future, experimentation should include wind speed measurements taken at the water surface so that more accurate transfer velocities can be calculated.

Given the above discussion on degassing it appears that the calculated IPCC flux is not only an overestimation but that the EF5-r factor for the LII was actually considerably < 0.0005 due to the dominant role played by degassing of antecedent N_2O. This is despite the potential for underestimating the flux with the chamber methodology used. In practice a discrete measurement of EF5-g is extremely difficult, requiring detailed and extensive resources to acquire knowledge on the presence of groundwater flows into a river and their respective dissolved N_2O concentrations. In most instances the antecedent N_2O contribution to a river flux measurement will be unknown. It has been previously indicated that denitrification in alluvial aquifers, where N_2O concentrations may be up to 100 times greater than the concentrations in the overlying river water, may contribute to dissolved N_2O concentrations in river water (MacMahon & Dennehey, 1999). Thus, as this study demonstrates, caution must be exercised in assigning N_2O fluxes from river surfaces solely to the EF5-r emission factor if contributions from EF5-g are present.

Of course river N_2O emissions could be treated as strictly that, i.e. the N_2O flux from the river system in question, since this is an easily definable area from which to take actual flux measurements. Then if the catchment's area and NO_3–N leaching load are known perhaps an amalgamated EF5 emission factor for the river system can be derived for the catchment concerned. In our study, neither the catchment's area nor the NO_3–N leaching load were readily definable due to the flat nature of the surrounding landscape and the unknown

groundwater contributions to the aquifer feeding the river. Further research needs be performed to derive the exact origins and potential processing of the N_2O in the LII river and this could be performed using isotopic studies.

Previously the few river studies that have measured N_2O fluxes directly have been performed on either large rivers (MacMahon & Dennehey, 1999, Cole & Caraco, 2001) or on a small agricultural stream (Hasegawa *et al.*, 2000). Clearly water residence times and river geometries vary and these in turn will influence the potential for in-stream processing of NO_3–N (Petersen *et al.*, 2001). For example, the residence time in the Hudson river study averaged 0.15 yr (Cole & Caraco, 2001) while in our study the estimated residence time was < 11 h. This short residence time may help to explain the relatively conserved NO_3–N loading in the LII, despite the continual presence of water soluble organic carbon. Further work is also required to assess the *in-situ* NO_3–N transformations in rivers such as the LII.

Our results may have significant implications for New Zealand's river systems given that the rivers are relatively short, by world standards, and will have short residence times when compared to those of other studies e.g. MacMahon & Dennehey (1999).

This study also reinforces the comments made by Reay et al.(2003), who cautioned against making total N_2O flux estimates for drainage waters based on measurements at widely spaced sampling points. Had we measured fluxes at only site 1 or only site 4 we would have obtained a misleading result. The cumulative data from four sites provides a more informed appraisal of the variation and magnitude of the fluxes, but clearly demonstrates the need for spatially intensive sampling. Clearly a key factor in determining where to measure river N_2O fluxes is the possible presence of contributing groundwater flows that may contain antecedent dissolved N_2O. This will depend on the hydrological network of the river source. Aquifer-fed rivers may behave differently to those rivers where significant contributions come from overland flows. Our study highlights the suggestion made that the

IPCC methodology for assessing indirect N_2O emissions be at least partially spatially explicit (Groffman *et al.*, 2002). River factors such as the ratio of depth: width, speed, gradient, residence time, and water sources should perhaps be considered. Our results also support the hypothesis that the IPCC methodology over-estimates the anthropogenic source of N_2O (Nevison, 2000b), at least with respect to the EF5 emission factor.

In summary our flux measurements from the river surface indicate significant degassing of antecedent N_2O with a relatively conserved NO_3–N loading. The measured N_2O fluxes, concentrations of dissolved N_2O, and N_2O–N: NO_3–N ratios were all within the range of previously reported values. Calculation of an EF5-r factor, based on the LII river NO_3–N load and measured N_2O–N fluxes yielded a result that was approximately 6.6% of the IPCC default EF5-r value. However, included in this calculation is a contribution from antecedent N_2O that should really be included in an EF5-g emission factor. Further work is required to separate out the magnitude of the N_2O–N fluxes from these two sources.

Acknowledgements

References

Bowden MJ (1986) *The Christchurch Artesian Aquifers: a report prepared by the resources division of the North Canterbury Catchment Board and Regional Water Board.* Christchurch, New Zealand., 159 pp.

Clesceri LS, Greenberg AE, Eaton AD (1998) *Standard Methods for the Examination of Water and Wastewater.* American Public Health Association, American Water Works Association, Water Environment Federation, Washington, D.C.

Cole JJ, Caraco NF (2001) Emissions of nitrous oxide (N_2O) from a tidal, freshwater river, the Hudson River, New York. *Environmental Science & Technology,* **35,** 991-996.

Davidson EA, Firestone MK (1988) Measurement of nitrous oxide dissolved in soil solution. *Soil Science Society of America Journal,* **52,** 1201-1203.

Davie T (2003) *Fundamentals of Hydrology.* Routledge, London and New York, 169 pp.

Dojlido JR, Best GA (1993) *Chemistry of water and water pollution.* Ellis Horwood, Chichester.

Dowdell RJ, Burford JR, Crees R (1979) Losses of nitrous oxide dissolved in drainage water from agricultural land. *Nature,* **278,** 342-343.

Groffman PM, Gold AJ, Addy K (2000) Nitrous oxide production in riparian zones and its importance to national emission inventories. *Chemosphere - Global Change Science,* **2,** 291-299.

Groffman PM, Gold AJ, Kellog DQ, Addy K (2002) Mechanisms, rates and assessment of N_2O in groundwater, riparian zones and rivers. In *Non-CO$_2$ Greenhouse Gases: Scientific Understanding, Control Options and Policy Aspects. Proceedings of the Third International Symposium, Maastricht, The Netherlands.* (eds van Ham J, Baede APM, Guicherit R, Williams-Jacobse JGFM), pp. 159-166. Millpress, Rotterdam.

Hasegawa K, Hanaki K, Matsuo T, Hidaka S (2000) Nitrous oxide from the agricultural water system contaminated with high nitrogen. *Chemosphere -Global Change Science,* **2,** 335-345.

Holmen K, Liss PS (1984) Models for air-water gas transfer: an experimental investigation. *Tellus Series B-Chemical & Physical Meteorology,* **36,** 92-100.

Inamder SP, Christopher SF, Mitchell MJ (2004) Export mechanisms for dissolved organic carbon and nitrate during summer storm events in a glaciated forested catchment in New York, USA. *Hydrological Processes,* **18,** 2651-2661.

IPCC (1997) *Guidelines for National Greenhouse gas Inventories.* OECD/OCDE, Paris.

Israelsen OW, Hansen VE (1962) *Irrigation Principles and Practices.* John Wiley and Sons Inc., New York.

Kirkwood DS (1992) Stability of solutions of nutrient salts during storage. *Marine Chemistry,* **38,** 151-164.

Liss PS (1973) Processes of gas exchange across an air-water interface. *Deep Sea Research,* **20,** 221-238.

Liss PS, Slater PG (1974) Flux of gases across the air-sea interface. *Nature,* **247,** 184-184.

MacIntyre S, Wanninkhof R, Chanton JP (1995) Trace gas exchange across the air-water interface in freshwater and coastal marine environments. In *Biogenic trace gas emissions: measuring emissions from soil and water.* (eds Matson PA, Harriss RC), pp. 52-97. Blackwell Science Inc., Cambridge, MA.

MacMahon PB, Dennehey KF (1999) N_2O emissions from a nitrogen-enriched river. *Environmental Science & Technology,* **33,** 21-25.

Mosier A, Kroeze C, Nevison C, Oenema O, Seitzinger S, Vancleemput O (1998) Closing the global N_2O budget: nitrous oxide emissions through the agricultural nitrogen cycle -

OECD/IPCC/IEA phase ii development of IPCC guidelines for national greenhouse gas inventory methodology. *Nutrient Cycling in Agroecosystems,* **52,** 225-248.

Mosier A, Mack L (1980) Gas chromatographic system for precise, rapid analysis of nitrous oxide. *Soil Science Society of America Journal,* **44,** 1121-1123.

Mosley MP, Jowett I, Tomlinson AI (1992) Data, Information and Engineering Applications. In *Waters of New Zealand* (ed Mosley MP), pp. 29-61. New Zealand Hydrological Society Incorporated, Wellington.

Nevison C (2000a) Good Practice Guidance and Uncertainty Management in National Greenhouse Gas Inventories. Indirect N_2O emissions from agriculture [Online]. [17 p]. Available at http://www.ipcc-nggip.iges.or.jp/public/gp/bgp/4_6_Indirect_N2O_Agriculture.pdf (modified 25 Feb. 2003; accessed April 2005) International Panel on Climate Change

Nevison C (2000b) Review of the IPCC methodology for estimating nitrous oxide emissions associated with agricultural leaching and runoff. *Chemosphere - Global Change Science,* **2,** 493-500.

New Zealand Climate Change Office (2004) *New Zealand's Greenhouse Gas Inventory 1990-2002:The National Inventory Report and Common Reporting Format Tables.* Ministry for the Environment, Wellington, 146 pp.

Petersen BJ, Wollheim WM, Mulholland PJ, *et al.* (2001) Control of nitrogen export from watersheds by headwater streams. *Science,* **292,** 86-90.

Prinn RG, Cunnold DM, Rasmussen RA, *et al.* (1990) Atmospheric emissions and trends of nitrous oxide deduced from 10 years of ALE/GAGE data. *Journal of Geophysical Research,* **95,** 18369-18385.

Reay DS, Smith KA, Edwards AC (2003) Nitrous oxide emission from agricultural drainage waters. *Global Change Biology,* **9,** 195-203.

Rockmann T, Kaiser J, Brenninkmeijer CAM (2003) The isotopic fingerprint of the pre-industrial and the anthropogenic N_2O source. *Atmospheric Chemistry and Physics,* **3,** 315-323.

Seitzinger S, Kroeze C (1998) Global distribution of nitrous oxide production and N inputs in fresh water and coastal marine ecosystems. *Global Biogeochemical Cycles,* **12,** 93-113.

Weiss RF, Price BA (1980) Nitrous Oxide Solubility in Water and Seawater. *Marine Chemistry,* **8,** 347-359.

Young CL (1981) *Oxides of nitrogen.* Pergamon Press, Oxford.

Table 1 Water velocities, river flow and residence times of the LII river at Site 4

Season	Date	Average water velocity $(m\ s^{-1})$	River flow $(m^3\ s^{-1})$	Residence time (h)
Fall	31-May	0.26	2.98	10.2
Winter	17-Jun	0.30	3.34	9.1
Winter	8-Jul	0.28	3.32	9.2
Winter	16-Aug	0.23	3.35	9.1
Spring	10-Sep	0.32	4.07	7.5

Table 2 Mean nitrate-N (NO_3-N) and ammonium concentrations (NH_4-N) in the LII river over time, standard error of the mean was < 0.01 in all cases (data not presented).

N form	Season	Date	Site 1	Site 2	Site 3	Site 4
NO_3-N	Fall	5th March	3.25	4.72	2.63	2.56
(mg L^{-1})		19th March	3.24	5.19	2.77	2.69
		5th April	3.07	3.36	2.86	2.29
		26th April	2.98	3.48	2.91	2.82
		3rd May	2.83	3.71	2.85	2.81
		17th May	2.88	3.59	2.95	2.95
		31st May	2.85	3.82	3.05	3.06
	Winter	17th June	2.83	4.11	2.95	2.88
		8th July	2.83	3.90	2.94	2.93
		28th July	2.91	3.73	2.85	2.88
		16th August	2.88	3.75	2.58	2.59
	Spring	10th September	2.92	3.80	2.82	3.12
		1st October	2.91	3.86	2.70	2.98
NH_4-N	Fall	5th March	0.06	0.06	0.12	0.06
(mg L^{-1})		19th March	0.01	0.01	0.06	0.03
		5th April	0.00	0.05	0.03	0.04
		26th April	0.01	0.05	0.05	0.05
		3rd May	0.01	0.01	0.02	0.02
		17th May	0.02	0.03	0.03	0.03
		31st May	0.04	0.03	0.03	0.03
	Winter	17th June	0.06	0.06	0.07	0.08
		8th July	0.04	0.02	0.04	0.04
		28th July	0.01	0.01	0.01	0.01
		16th August	0	0.02	0.08	0.11
	Spring	10th September	0	0	0	0
		1st October	0	0	0	0

Table 3 Mean dissolved N_2O-N concentrations (μg N_2O-N L^{-1}); $n = 3$ numbers in brackets are standard error of the mean) and dissolved N_2O-N: NO_3-N ratios.

	Season	Date	Site 1	Site 2	Site 3	Site 4
Dissolved N_2O-N	Fall	5th Apr.	1.37 (0.11)	1.09 (0.12)	0.77 (0.07)	0.54 (0.06)
		26th Apr.	1.43 (0.01)	1.08 (0.17)	1.06 (0.16)	1.10 (0.18)
		3rd May	1.04 (0.42)	1.27 (0.03)	0.74 (0.03)	0.65 (0.01)
		17th May	1.11 (0.46)	1.38 (0.06)	0.79 (0.04)	0.69 (0.01)
		31st May	1.26 (0.28)	0.76 (0.55)	0.68 (0.06)	0.49 (0.01)
	Winter	17th Jun.	1.89 (0.12)	1.88 (0.01)	0.88 (0.02)	0.73 (0.01)
		8th Jul.	1.35 (0.03)	1.12 (0.04)	0.51 (0.01)	0.45 (0.01)
		28th Jul.	1.21 (0.04)	1.12 (0.01)	0.52 (0.01)	0.43 (0.01)
		16th Aug.	1.49 (0.03)	1.94 (0.03)	0.81 (0.26)	0.94 (0.01)
	Spring	10th Sep.	1.68 (0.05)	1.50 (0.02)	0.65 (0.01)	0.52 (0.01)
Ratio N_2O-N: NO_3-N	Fall	5th Apr.	0.00045	0.00032	0.00027	0.00024
		26th Apr.	0.00048	0.00031	0.00036	0.00039
		3rd May	0.00037	0.00034	0.00026	0.00023
		17th May	0.00039	0.00038	0.00027	0.00023
		31st May	0.00044	0.00020	0.00022	0.00016
	Winter	17th Jun.	0.00067	0.00046	0.00030	0.00025
		8th Jul.	0.00048	0.00029	0.00017	0.00015
		28th Jul.	0.00041	0.00030	0.00018	0.00015
		16th Aug.	0.00052	0.00052	0.00032	0.00036
	Spring	10th Sep.	0.00057	0.00040	0.00023	0.00017

Table 4. Mean dissolved N_2O-N fluxes ($\mu g\ m^{-2}\ h^{-1}$). Numbers in brackets are standard errors of the mean, $n = 3$.

Season	Date	Site 1	Site 2	Site 3	Site 4
Fall	3rd May	307 (28)	173 (44)	179 (15)	90 (7)
	17th May	109 (6)	223 (7)	151 (10)	119 (5)
	31st May	299 (13)	320 (14)	78 (6)	89 (6)
Winter	17th June	183 (12)	311 (30)	139 (9)	131 (7)
	8th July	93 (8)	241 (12)	90 (2)	75 (2)
	16th August	211 (10)	272 (4)	195 (6)	124 (9)
Spring	10th September	188 (10)	173 (10)	106 (6)	138 (4)

Figure Legends

Fig. 1 Map showing global and regional locality of the study site.

Fig. 2 Meteorological data recorded at a distance of 3 km from site 1.

Fig. 3 Dissolved water soluble carbon concentrations in the LII river water over time at each site. Numerals in the legend refer to site number while OC and IC refer to organic and inorganic carbon respectively.

Fig. 4 The relationship between N_2O–N fluxes and NO_3–N concentrations for the LII river (sites 1 to 4), Avon, Heathcote and Halswell rivers, 7 sample dates (Fig 4a); and the relationship between dissolved N_2O and the NO_3–N concentrations for the LII river, 10 sample dates (Fig. 4b)

Fig.5 Relationship between the mean N_2O–N fluxes and mean dissolved N_2O concentrations for sites 1 to 4. Error bars are $\pm$ standard error of the mean, y axis $n = 10$, x axis $n = 3$). Also shown are the equilibrium concentrations of N_2O in the river water and the predicted N_2O fluxes at N_2O transfer velocities (V^{N2O})of 2.28 x10^{-4} (solid line) and 3.65 x10^{-5} m s^{-1} (dotted line).
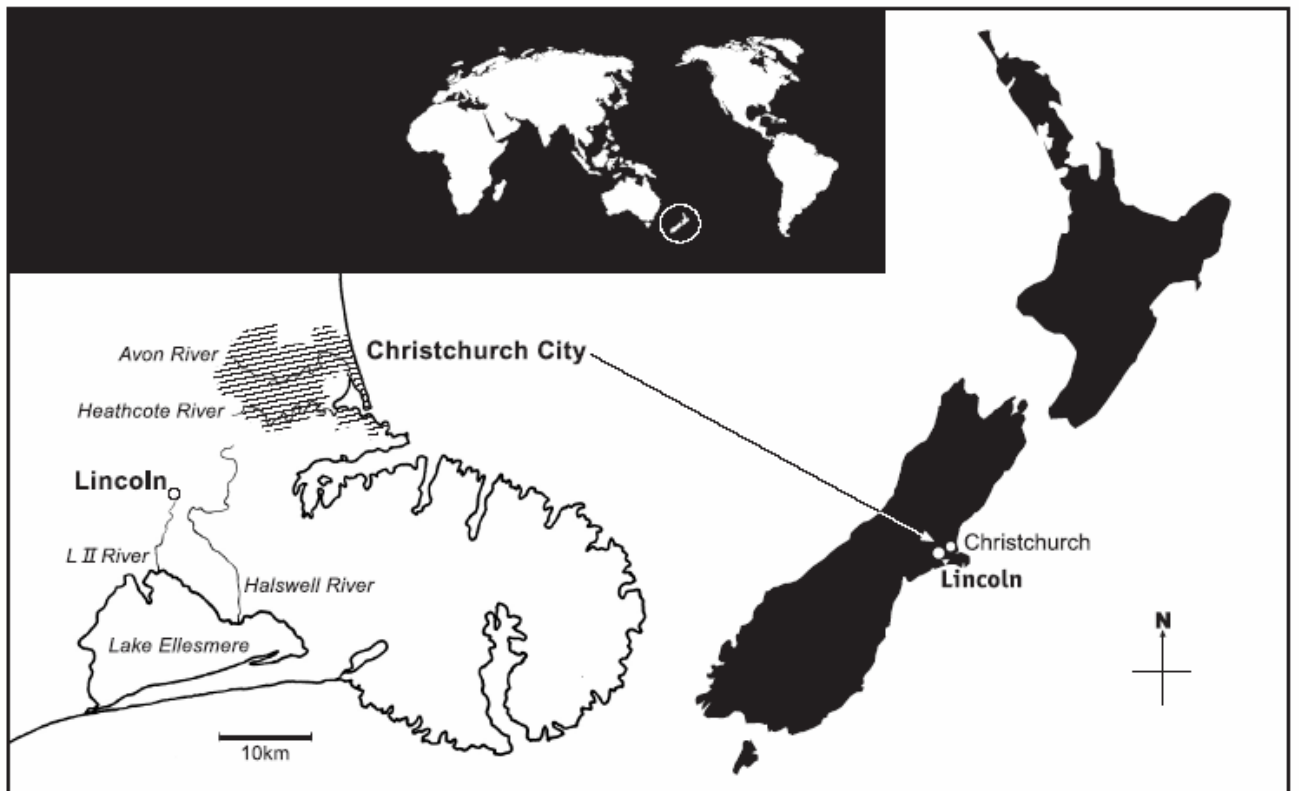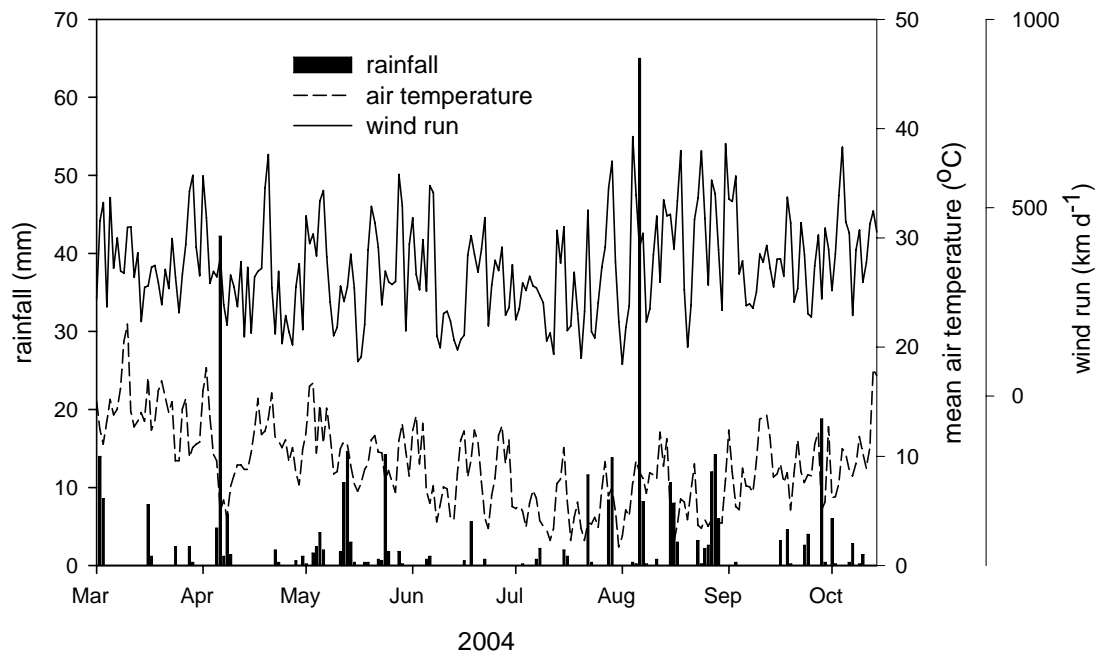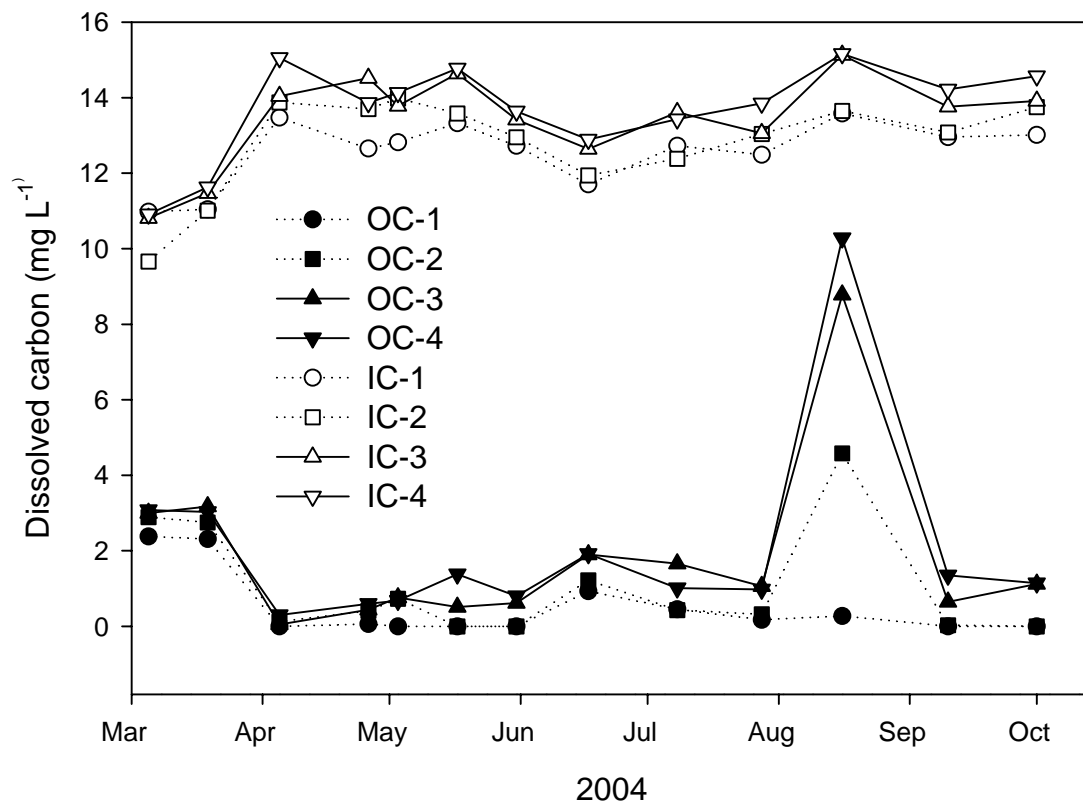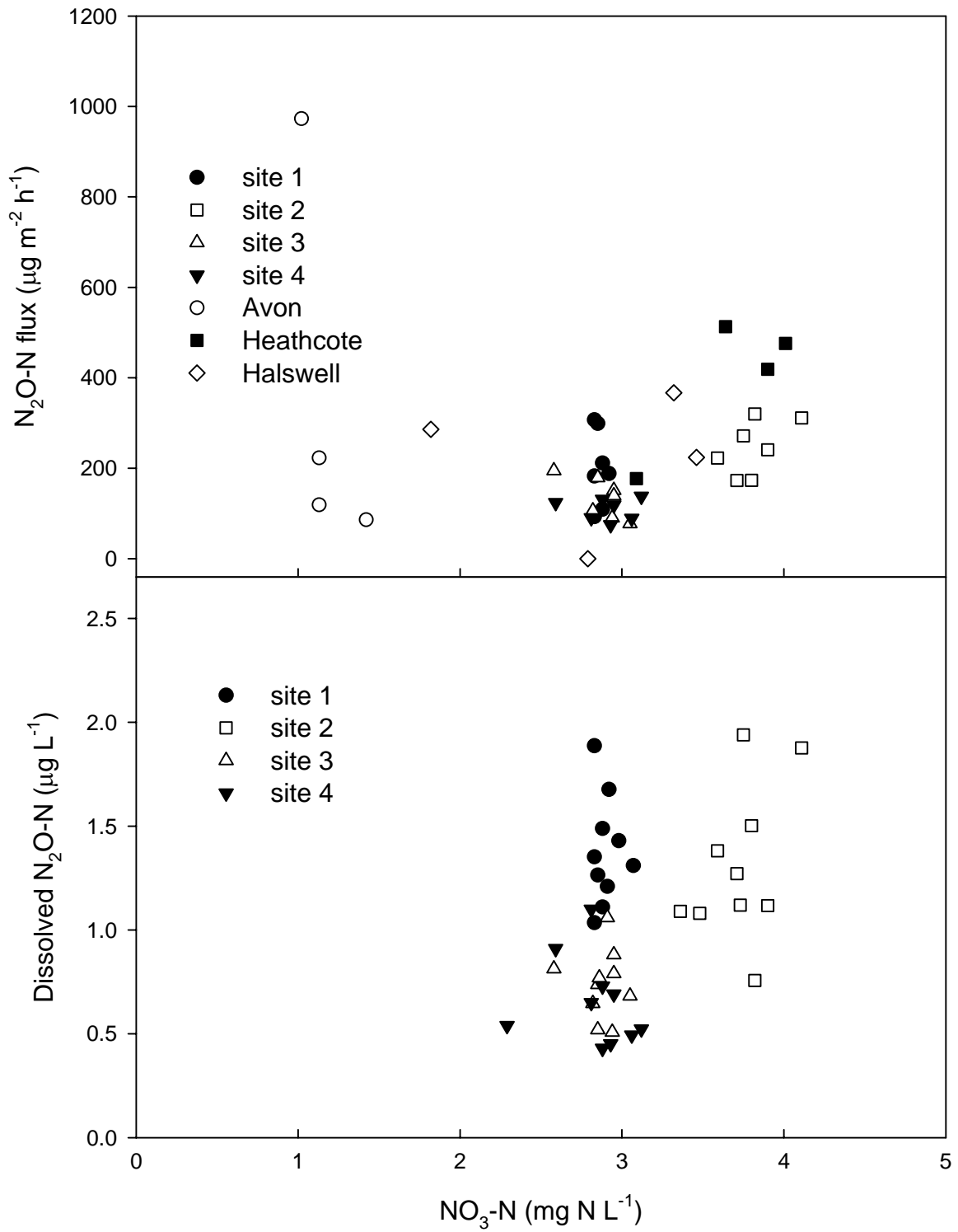
Figure 1

Figure 2

Figure 3

Figure 4

Figure 5